miR-200c-3p spreads invasive capacity in human oral squamous cell carcinoma microenvironment

Kawakubo, Tomoyo
Department of Immunological and Molecular Pharmacology, Faculty of Pharmaceutical Science, Fukuoka University

Morioka, Masahiko
Department of Immunological and Molecular Pharmacology, Faculty of Pharmaceutical Science, Fukuoka University

Hazekawa, Mai
Department of Immunological and Molecular Pharmacology, Faculty of Pharmaceutical Science, Fukuoka University

Yasukochi, Atsushi
Section of Oral and Maxillofacial Oncology, Division of Maxillofacial Diagnostic and Surgical Sciences, Faculty of Dental Science, Kyushu University

他

出版情報：Molecular Carcinogenesis. 57 (2), pp.295-302, 2017-10-05. Wiley
バージョン：

BRIEF COMMUNICATION

miR-200c-3p spreads invasive capacity in human oral squamous cell carcinoma microenvironment†

Abbreviated title: miR200c-3p accelerates invasion in oral cancer

Tomoyo Kawakubo-Yasukochi[1*], Masahiko Morioka[1,2], Mai Hazekawa[1], Atsushi Yasukochi[2], Takuya Nishinakagawa[1], Kazuhiko Ono[1], Shintaro Kawano[2], Seiji Nakamura[2], Manabu Nakashima[1]

[1]Department of Immunological and Molecular Pharmacology, Faculty of Pharmaceutical Science, Fukuoka University, 8-19-1 Nanakuma, Jonan-ku, Fukuoka 814-0180, Japan;

[2]Section of Oral and Maxillofacial Oncology, Division of Maxillofacial Diagnostic and Surgical Sciences, Faculty of Dental Science, Kyushu University, 3-1-1 Maidashi, Higashi-ku, Fukuoka 812-8582, Japan

***Correspondence**: Tomoyo Kawakubo-Yasukochi, DDS, PhD, Department of Immunological and Molecular Pharmacology, Faculty of Pharmaceutical Science, Fukuoka University, 8-19-1 Nanakuma, Jonan-ku, Fukuoka 814-0180, Japan, Tel: +81-92-871-6631, Email: tomoyoyasu@fukuoka-u.ac.jp

Funding:

This work was supported by the Japan Society for the Promotion of Science (KAKENHI grant no. 17H01603 to S.N., 26861554 and 16K11496 to T.K-Y., 16K20585 to A.Y.), the Central Research Institute of Fukuoka University (no. 157103 to T.K-Y. and M.H.), the Ichiro Kanehara Foundation (no. 16KI059 to T.K-Y.), and the Shin-Nihon of Advanced Medical Research (to T.K-Y.).

†This article has been accepted for publication and undergone full peer review but has not been through the copyediting, typesetting, pagination and proofreading process, which may lead to differences between this version and the Version of Record. Please cite this article as doi: [10.1002/mc.22744]

Additional Supporting Information may be found in the online version of this article.

Received 18 July 2017; Revised 18 September 2017; Accepted 29 September 2017
Molecular Carcinogenesis

DOI 10.1002/mc.22744

Abbreviations:

Epithelial-to-mesenchymal transition, EMT

MicroRNAs, miRNAs

Oral squamous cell carcinoma, OSCC

RNA-induced silencing complex, RISC

Untranslated region, UTR

Abstract

Oral squamous cell carcinoma (OSCC) constitutes over 90% of all cancers in the oral cavity. The prognosis for patients with invasive OSCC is poor; therefore, it is important to understand the molecular mechanisms of invasion and subsequent metastasis not only to prevent cancer progression but also to detect new therapeutic targets against OSCC. Recently, extracellular vesicles—particularly exosomes—have been recognized as intercellular communicators in the tumor microenvironment. As exosomic cargo, deregulated microRNAs (miRNAs) can shape the surrounding microenvironment in a cancer-dependent manner. Previous studies have shown inconsistent results regarding miR-200c-3p expression levels in OSCC cell lines, tissues, or serum—likely because of the heterogeneous characters of the specimen materials. For this reason, single-cell clone analyses are necessary to effectively assess the role of exosome-derived miRNAs on cells within the tumor microenvironment. The present study utilized integrated microarray profiling to compare exosome-derived miRNA and exosome-treated cell-derived mRNA expression. Data were acquired from noninvasive SQUU-A and highly invasive SQUU-B tongue cancer cell clones derived from a single patient to determine candidate miRNAs that promote OSCC invasion. Matrigel invasion assays confirmed that hsa-miR-200c-3p was a key pro-invasion factor among six miRNA candidates. Consistently, silencing of the miR-200c-3p targets, *CHD9* and *WRN,* significantly accelerated the invasive potential of SQUU-A cells. Thus, our data indicate that miR-200c-3p in exosomes derived from a highly invasive OSCC line can induce a similar phenotype in non-invasive counterparts.

Key words: microRNA, invasion, microarray, tumor microenvironment

Introduction

Oral squamous cell carcinoma (OSCC) is the most common form of oral cancer with a high potential for local invasion and lymph node metastasis[1]. Despite an increasing prevalence on a global scale, the overall 5-year survival rate has not significantly changed during the past 30 years[2,3].

OSCC development results from an accumulation of genetic alterations[1]. Recent studies demonstrate that non-coding RNAs—such as microRNAs (miRNAs)—can exhibit either tumor-suppressive or oncogenic functions in OSCC progression[1,2,4]. miRNAs are short (18–25 nucleotides), single-stranded, non-coding RNAs that bind complementary sequences typically present in the 3' untranslated region (UTR) of the target mRNAs, which blocks their translation by subsequent recruitment of the RNA-induced silencing complex (RISC)[5,6]. Given that over 60% of human genes are predicted to be regulated by this process, miRNAs likely govern all cellular, physiological, and developmental processes[7]. Consequentially, aberrant miRNA expression is common in various cancers, and miRNA signatures have been helpful as diagnostic, prognostic, and therapeutic biomarkers for cancers, including OSCC [8].

The majority of miRNA expression profiling studies have used either cancer cell lines[9,10] or tissue samples[4,11-18]; however, the resulting data were always controversial when discussing the role of individual miRNAs[4]. Several factors are likely responsible for these inconsistencies, including methodological and statistical variation, as well as the presence of heterogeneous expression patterns in OSCC cell lines and tumor tissue samples[1,19,20].

Exosomes are small membrane vesicles (30–100 nm) derived from the luminal membranes of multivesicular bodies and constitutively released via fusion with the cell membrane[21-23]. Notably, these vesicles mediate local and systemic cell communication through the horizontal transfer of their cargo, which includes proteins, lipids, DNAs, miRNAs, and mRNAs protected from protease and RNase-mediated degradation by the surrounding lipid bilayer[21-23]. Exosome release has been demonstrated in many proliferating cell types and detected in various body fluids, such as serum, urine, and saliva. In addition, tumor cells show a marked increase in exosome release, as evidenced by their elevated presence in the plasma, ascites, and pleural effusions of cancer patients[24,25]. Therefore, exosome analysis may serve as a powerful diagnostic and therapeutic tool and uncover a new landscape for miRNAs in cancer therapy.

Our group performed an integrated miRNA/mRNA analysis using non-metastatic SQUU-A and metastatic SQUU-B tongue cancer cell lines isolated from the same patient[26,27]. Notably, metastatic OSCC cells were capable of inducing an invasive phenotype in non-metastatic counterparts via miR-200c-3p, providing clear insights into the function of this miRNA in the OSCC microenvironment.

Results and Discussion

Integrated expression profiling between exosome-derived miRNAs and mRNAs in exosome-treated SQUU-A cells

We previously demonstrated that exosome-mediated crosstalk determines invasiveness and organotropic metastasis in OSCC using SQUU-A and SQUU-B cell lines[27,28], and Matrigel invasion assays confirmed the malignant potential of SQUU-B but not SQUU-A cells (Supplementary Figure 1)[22]. miRNAs have attracted the most attention of any exosome cargo because of their regulatory roles in gene expression. Interestingly, miRNAs are selectively incorporated and relatively more abundant in exosomes than in their parent cells[18,29]. Accordingly, exosomes were obtained from SQUU-A and SQUU-B cell culture supernatants—henceforth referred to as ExoA and ExoB, respectively—and analyzed for their miRNA expression profiles. The resulting data showed 21 significantly upregulated and 11 downregulated miRNAs in ExoB as compared to ExoA (Table 1).

A subsequent transcriptome array was performed to examine differential mRNA expression patterns in SQUU-A cells treated with ExoB compared to those treated with ExoA, which identified seven upregulated and 15 downregulated mRNAs (Table 2). Combining the miRNA and mRNA analyses revealed seven mRNAs likely regulated by exosome miRNAs: *TRIB3* by miR-205-5p, *FRK* by miR-23b-3p and miR-191-5p, *WRN* by miR-200c-3p and miR-221-3p, *ETNK1* by miR-200c-3p, *CHD9* by miR-200c-3p, *PANK2* by miR-23b-3p, and *AKT3* by miR-92b-5p (Table 2). These results were also validated by qRT-PCR analysis (Supplementary Figure 2a,b) using the primer set shown in Supplementary Table 1.

miR-200c-3p regulates invasive potential in OSCC cells

We next examined whether any of the six identified miRNAs (miR-23b-3p, miR-92b-5p, miR-191-5p, miR-200c-3p, miR-205-5p, and miR-221-3p) and seven downstream mRNAs (*TRIB3*, *FRK*, *WRN*, *ETNK1*, *CHD9*, *PANK2*, and *AKT3*) were able to induce invasion in SQUU-A cells. After qRT-PCR validation of each miRNA (Figure 1a) or its downstream mRNAs—*TRIB3*, *ERBB3*[30], and *ZEB1*[30] for miR-205-5p and *CHD9*, *ETNK1*, and *WRN* for miR200c-3p (Figure 1b–d)—to check the transfer efficiency of miRNA mimic or inhibitor nucleotides (Supplementary Table 2), Matrigel invasion assays were performed using cells individually transfected with a miRNA mimic or inhibitor of each of the six miRNAs. Although it was difficult to regulate gene transfer efficiency at the same levels shown in miRNA arrays and validation data (Table 1, Supplementary Figure 2a), SQUU-A cells showed a 50.9-fold increase in miR200c-3p expression as compared with that in controls and a significantly accelerated invasive capacity (Figure 1e). Conversely, SQUU-B cells transfected with the miR-200c-3p inhibitor showed a 3.70-fold decrease in the number of invasive cells (Figure 1e).

However, no changes in invasive potential were observed in SQUU-A cells transfected with the miR-23b-3p, miR-92b-5p, miR-191-5p, or miR-221-3p mimics or the miR-205-5p inhibitor.

Since miRNAs predominantly act through translational inhibition[5-7,31], we subsequently focused on the miR-200c-3p downstream targets *CHD9*, *ETNK1*, and *WRN* (Table 2). Notably, qRT-PCR validation analysis also revealed that SQUU-A cells transfected with miR200c-3p mimic showed decreased *CHD9* (0.38-fold), *ETNK1* (0.30-fold), and *WRN* (0.63-fold) mRNA expression compared to those transfected with the mimic negative control (Figure 1d). Correspondingly, increased *CHD9* (1.28-fold), *ETNK1* (1.73-fold), and *WRN* (1.99-fold) expression was observed in SQUU-B cells transfected with miR200c-3p inhibitor as compared to that in negative controls (Figure 1c). Thus, to examine whether these three miR-200c-3p target genes mediated miR-200c-3p-dependent invasive potential, we examined differences in invasive capacity between SQUU-A and SQUU-B cells in terms of protein expression levels. In SQUU-A cells, siRNAs effectively reduced the targeted mRNA and protein levels (Figure 2a,b and Supplementary Table 3). Furthermore, Matrigel invasion assay analysis revealed that SQUU-A cells transfected with *CHD9* and *WRN* siRNAs displayed significantly accelerated invasion as compared to those transfected with negative control siRNA; however, no differences were observed with regards to *ETNK1* (Figure 2c). Conversely, SQUU-B cells transfected with *CHD9* or *WRN* exhibited a significant decrease in invasion, whereas no marked changes were observed with *ETNK1*-overexpressing SQUU-B cells (Figure 2d,e). Collectively, these findings suggest that the spread of the invasive potential between OSCC cell clones could be driven by exosome-derived miR-200c-3p and its effect on *CHD9* and *WRN* expression in the same tumor mass.

CHD9 (also known as CReMM) is an ATP-dependent chromatin remodeling enzyme that binds skeletal tissue-specific promoters to regulate the expression of genes such as *RUNX2* (Runt-related transcription factor 2), *BGN* (biglycan), *BGLAP* (bone gamma-carboxyglutamate Gla protein), and *MYH6* (α-myosin heavy chain)[32]. Previous work indicates that CDH9 inactivation facilitates metastatic spread to the bone in neuroblastoma[33]. In addition, up to 50% of OSCC cases show invasion into the maxilla or mandible at presentation[34]. In support of this, our data demonstrate that *CHD9* acts to suppress cell invasion (Figure 2c), although the specific mechanism remains unclear.

In contrast, WRN is a member of the RecQ helicase family and plays an important role in maintaining genomic stability[35]. *WRN* loss-of-function mutations result in Werner syndrome, an inherited disorder characterized by premature aging, genomic instability, and increased early-onset cancer incidence[36,37]. Decreased WRN expression may cause genomic instability in normal cells and induce tumor initiation[36]. Meanwhile, malignant cells often acquire increased WRN expression to protect their own genomic stability[36], although its promoter is often hypermethylated[38]. Moreover, some studies demonstrate that *WRN* silencing hinders cell viability and leads to mitotic catastrophe in several types of cancer[35,37], including head and neck cancers[39]. In our study, *WRN*-knockdown SQUU-A cells showed no differences in morphology or cell viability 24 h after transfection (data not shown), but a marked increase in invasive potential was observed (Figure 2a–c). In addition, its overexpression attenuated the invasion of SQUU-B cells. Based on these results, we propose that *WRN* acts as a tumor suppressor to prevent OSCC invasion, likely as a regulator of genome stability.

ETNK1 is a miR-200c-3p target also detected in our integrated miRNA/mRNA microarray analysis (Table 2). ETNK1 catalytic activity is involved in atypical chronic myeloid leukemia and chronic myelomonocytic leukemia progression[40]. While its role in solid cancer progression has not been studied, our data suggest that ETNK1 expression is unrelated to OSCC invasion (Figure 2c,e).

Many previous reports have indicated that miR-200c attenuates cell invasion and metastasis by downregulating the master regulators of the epithelial-to-mesenchymal transition (EMT)—such as ZEB1 and ZEB2—in several cancers[17,41-43], including head and neck cancer[44]. In contrast, other studies propose that increased miR-200c expression is an indicator of malignancy, as it is often found to be overexpressed in the sera of cancer patients as compared with levels in healthy controls[45,46]. Le *et al*. demonstrated the miR-200 family-containing extracellular vesicles are enriched in the sera of patients with metastatic cancers and ectopic expression of miR-200 family members can enhance the metastatic ability of tumor cells in some settings via the novel miR-200c targets TKS5 (SH3PXD2A; SH3 and PX domains 2A) and MYLK (MLCK; myosin light chain kinase)[47]. There was no significant difference in the expression levels of the miR-200 targets *ZEB1*, *ZEB2*, *TKS5*, and *MYLK* between SQUU-A cells treated with ExoB and those treated with ExoA in our differential mRNA array (Table 2); however, we did not investigate the endogenous expression of these targets in the unique two-cell line model in the present study.

Intratumoral heterogeneity is a general characteristic of malignant tumors and represents a major obstacle in the study of tumor biology, and miRNA analyses are no exception. The abovementioned previous studies of the effects of miR-200c family members on metastasis also suffer from issues related to tumor heterogeneity. This heterogeneity may influence measurements of miRNA expression, and consequently, the number of samples are tended to be interpreted as representative estimates. In addition, conflicting correlations between amounts of intracellular and extracellular (circulating) miRNAs have been observed in cancer patients[48], and recent studies indicate that circulating miRNAs may be potential biomarkers for malignant diseases[45-48]. In fact, our study indicates the existence of multiple OSCC cell types in a single tumor mass that secrete exosomes containing a unique set of miRNAs. Through the use of two unique malignant cell clones and the analysis of exosome-derived miRNAs, this study indicates that miR-200c-3p is an oncogenic miRNA capable of inducing invasive potential in noninvasive cells within an OSCC tumor mass.

Conflict of interest

The authors have no conflicts of interest to disclose.

Acknowledgements

The authors thank Dr. Kaori Yasuda (Cell Innovator Co., Ltd.) for assistance with microarray data analysis and useful discussion.

References

1. Sasahira T, Kirita T, Kuniyasu H. Update of molecular pathobiology in oral cancer: a review. *Int J Clin Oncol* 2014;19:431-436.
2. Choi S, Myers JN. Molecular pathogenesis of oral squamous cell carcinoma: implications for therapy. *J Dent Res* 2008;87:14-32.
3. Marsh D, Suchak K, Moutasim KA, Vallath S, Hopper C, Jerjes W, Upile T, Kalavrezos N, Violette SM, Weinreb PH, Chester KA, Chana JS, Marshall JF, Hart IR, Hackshaw AK, Piper K, Thomas GJ. Stromal features are predictive of disease mortality in oral cancer patients. *J Pathol* 2011;223:470-481.
4. Sethi N, Wright A, Wood H, Rabbitts P. MicroRNAs and head and neck cancer: reviewing the first decade of research. *Eur J Cancer* 2014;50:2619-2635.
5. Bartel DP. MicroRNAs: target recognition and regulatory functions. *Cell* 2009;136:215-233.
6. Chekulaeva M, Filipowicz W. Mechanisms of miRNA-mediated post-transcriptional regulation in animal cells. *Curr Opin Cell Biol* 2009;21:452-460.
7. Jansson MD, Lund AH. MicroRNA and cancer. *Mol Oncol* 2012;6:590-610.
8. Calin GA, Croce CM. MicroRNA signatures in human cancers. *Nat Rev Cancer* 2006;6:857-866.
9. Kozaki K, Imoto I, Mogi S, Omura K, Inazawa J. Exploration of tumor-suppressive microRNAs silenced by DNA hypermethylation in oral cancer. *Cancer Res* 2008;68:2094-2105.
10. Tran N, McLean T, Zhang X, Zhao CJ, Thomson JM, O'Brien C, Rose B. MicroRNA expression profiles in head and neck cancer cell lines. *Biochem Biophys Res Commun* 2007;358:12-17.
11. Manikandan M, Deva Magendhra Rao AK, Arunkumar G, Manickavasagam M, Rajkumar KS, Rajaraman R, Munirajan AK. Oral squamous cell carcinoma: microRNA expression profiling and integrative analyses for elucidation of tumorigenesis mechanism. *Mol Cancer* 2016;15:28.
12. Tseng HH, Tseng YK, You JJ, Kang BH, Wang TH, Yang CM, Chen HC, Liou HH, Liu PF, Ger LP, Tsai KW. Next-generation sequencing for microRNA profiling: microRNA-21-3p promotes oral cancer metastasis. *Anticancer Res* 2017;37:1059-1066.
13. Soga D, Yoshida S, Shiogama S, Miyazaki H, Kondo S, Shintani S. MicroRNA expression profiles in oral squamous cell carcinoma. *Oncol Rep* 2013;30:579-583.
14. Gombos K, Horváth R, Szele E, Juhász K, Gocze K, Somlai K, Pajkos G, Ember I, Olasz L. miRNA expression profiles of oral squamous cell carcinomas. *Anticancer Res* 2013;33:1511-1517.
15. Hung PS, Tu HF, Kao SY, Yang CC, Lui CJ, Huang TY, Chang KW, Lin SC. miR-31 is upregulated in oral premalignant epithelium and contributes to the immortalization of normal oral keratinocytes. *Carcinogenesis* 2014;35:1162-1171.

16. Huang WC, Chan SH, Jang TH, Chang JW, Ko YC, Yen TC, Chiang SL, Chiang WF, Shieh TY, Liao CT, Juang JL, Wang HC, Cheng AJ, Lu YC, Wang LH. miRNA-491-5p and GIT1 serve as modulators and biomarkers for oral squamous cell carcinoma invasion and metastasis. *Cancer Res* 2014;74:751-764.
17. Johnson JJ, Miller DL, Jiang R, Lui Y, Shi Z, Tarwater L, Williams R, Balsara R, Sauter ER, Stack MS. Protease-activated receptor-2-mediated NF-κB activation suppresses inflammation-associated tumor suppressor microRNAs in oral squamous cell carcinoma. *J Biol Chem* 2016;291:6936-6945.
18. Goldie BJ, Dun MD, Lin M, Smith ND, Verrillis NM, Dayas CV. Activity-associated miRNA are packaged in Map1b-enriched exosomes released from depolarized neurons. *Nucleic Acids Res* 2014;42:9195-9208.
19. Shiga K, Ogawa T, Katagiri K, Yoshida F, Tateda M, Matsuura K, Kobayashi T. Differences between oral cancer and cancers of the pharynx and larynx on a molecular level. *Oncol Lett* 2012;3:238-243.
20. Gupta GP, Massagué J. Cancer metastasis: building a framework. *Cell* 2006;127:679-695.
21. Peinado H, Alečković M, Lavotshkin S, Matei I, Costa-Silva B, Moreno-Bueno G, Hergueta-Redondo M, Williams C, García-Santos G, Ghajar C, Nitadori-Hoshino A, Hoffman C, Badal K, Garcia BA, Callahan MK, Yuan J, Martins VR, Skog J, Kaplan RN, Brady MS, Wolchok JD, Chapman PB, Kang Y, Bromberg J, Lyden D. Melanoma exosomes educate bone marrow progenitor cells toward a prometastatic phenotype through MET. *Nat Med* 2012;18:883-891.
22. Trajkovic K, Hsu C, Chiantia S, Rajendran L, Wenzel D, Wieland F, Schwille P, Brügger B, Simons M. Ceramide triggers budding of exosome vesicles into multivesicular endosomes. *Science* 2008;319:1244-1247.
23. Valadi H, Ekstrom K, Bossios A, Sjostrand M, Lee JJ, Lotvall JO. Exosome-mediated transfer of mRNAs and microRNAs is a novel mechanism of genetic exchange between cells. *Nat Cell Biol* 2007;9:654-659.
24. Andre F, Schartz NE, Movassagh M, Flament C, Pautier P, Morice P, Pomel C, Lhomme C, Escudier B, Le Chevalier T, Tursz T, Amigorena S, Raposo G, Angevin E, Zitvogel L. Malignant effusions and immunogenic tumour-derived exosomes. *Lancet* 2002;360:295-305.
25. Valenti R, Huber V, Filipazzi P, Pilla L, Sovena G, Villa A, Corbelli A, Fais S, Parmiani G, Rivoltini L. Human tumor-released microvesicles promote the differentiation of myeloid cells with transforming growth factor-mediate suppressive activity on T lymphocytes. *Cancer Res* 2006;66:9290-9298.
26. Morifuji M, Taniguchi S, Sakai H, Nakabeppu Y, Ohishi M. Differential expression of

cytokeratin after orthotopic implantation of newly established human tongue cancer cell lines of defined metastatic ability. *Am J Pathol* 2000;156:1317-1326.

27. Kawakubo-Yasukochi T, Morioka M, Hayashi Y, Nishinakagawa T, Hazekawa M, Kawano S, Nakamura S, Nakashima, M. The SQUU-B cell line spreads its metastatic properties to nonmetastatic clone SQUU-A from the same patient through exosomes. *J Oral Biosci* 2016;58:33-38.
28. Morioka M, Kawakubo-Yasukochi T, Hayashi Y, Hazekawa M, Nishinakagawa T, Ono K, Kawano S, Nakamura S, Nakashima M. Exosomes from oral squamous carcinoma cell lines, SQUU-A and SQUU-B, define the tropism of lymphatic dissemination. *J Oral Biosci* 2016;58:180-184.
29. Guduric-Fuchs J, O'Connor A, Camp B, O'Neill CL, Medina RJ, Simpson DA. Selective extracellular vesicle-mediated export of an overlapping set of microRNAs from multiple cell types. *BMC Genomics* 2012;13:357.
30. De Cola A, Volpe S, Budani MC, Ferracin M, Lattanzio R, Turdo A, D'Agostino D, Capone E, Stassi G, Todaro M,Di Ilio C, Sala G, Piantelli M, Negrini M, Veronese A, De Laurenzi V. miR-205-5p-mediated downregulation of ErbB/HER receptors in breast cancer stem cells results in targeted therapy resistance. *Cell Death Dis* 2015;6:e1823.
31. Djuranovic S, Nahvi A, Green R. miRNA-mediated gene silencing by translational repression followed by mRNA deadenylation and decay. *Science* 2012;13:237-240.
32. Hall JA, Georgel PT. CHD proteins: a diverse family with strong ties. *Biochem Cell Biol* 2007;85:463-476.
33. Lasorsa VA, Formicola D, Pignataro P, Cimmino F, Calabrese FM, Mora J, Esposito MR, Pantile M, Zanon C, De Mariano M, Longo L, Hogarty MD, de Torres C, Tonini GP, Iolascon A, Capasso M. Exome and deep sequencing of clinically aggressive neuroblastoma reveal somatic mutations that affect key pathways involved in cancer progression. *Oncotarget* 2016;7:21840-21852.
34. Lubek JE, Magliocca KR. Evaluation of the bone margin in oral squamous cell carcinoma. *Oral Maxillofac Surg Clin North Am*. E-pub ahead of print 24 May 2017; doi: 10.1016/j.coms.2017.03.005.
35. Orlovetskie N, Serruya R, Abboud-Jarrous G, Jarrous N. Targeted inhibition of WRN helicase, replication stress and cancer. *Biochim Biophys Acta* 2017;1867:42-48.
36. Futami K, Furuichi Y. RECQL1 and WRN DNA repair helicases: potential therapeutic targets and proliferative markers against cancers. *Front Genet* 2015;5:441.
37. Hickson ID. RecQ helicases: caretakers of the genome. *Nat Rev Cancer* 2003;3:169-178.
38. Agrelo R, Cheng WH, Setien F, Ropero S, Espada J, Fraga MF, Herranz M, Paz MF,

Sanchez-Cespedes M, Artiga MJ, Guerrero D, Castells A, von Kobbe C, Bohr VA, Esteller M. Epigenetic inactivation of the premature aging Werner syndrome gene in human cancer. *Proc Natl Acad Sci U S A* 2006;103:8822-8827.

39. Arai A, Chano T, Futami K, Furuichi Y, Ikebuchi K, Inui T, Tameno H, Ochi Y, Shimada T, Hisa Y, Okabe H. RECQL1 and WRN proteins are potential therapeutic targets in head and neck squamous cell carcinoma. *Cancer Res* 2011;71:4598-4607.
40. Kosmider O. Mutation of ETNK1 in aCML and CMML. *Blood* 2015;125:422-423.
41. Wong CM, Wei L, Au SL, Fan DN, Zhou Y, Tsang FH, Law CT1, Lee JM, He X, Shi J, Wong CC, Ng IO. MiR-200b/200c/429 subfamily negatively regulates Rho/ROCK signaling pathway to suppress hepatocellular carcinoma metastasis. *Oncotarget* 2015;6:13658-13670.
42. Hur K, Toiyama Y, Takahashi M, Balaguer F, Nagasaka T, Koike J, Hemmi H, Koi M, Boland CR, Goel A. MicroRNA-200c modulates epithelial-to mesenchymal transition (EMT) in human colorectal cancer metastasis. *Gut* 2013;62:1315-1326.
43. Li H, Xu L, Li C, Zhao L, Ma Y, Zheng H, Li Z, Zhang Y, Wang R, Liu Y, Qu X. Ubiquitin ligase Cbl-b represses IGF-I-induced epithelial mesenchymal transition via ZEB2 and microRNA-200c regulation in gastric cancer cells. *Mol Cancer* 2014;13:136.
44. Lo WL, Yu CC, Chiou GY, Chen YW, Huang PI, Chien CS, Tseng LM, Chu PY, Lu KH, Chang KW, Kao SY, Chiou SH. MicroRNA-200c attenuates tumour growth and metastasis of presumptive head and neck squamous cell carcinoma stem cells. *J Pathol* 2011;223:482-495.
45. Zhang HP, Sun FB, Li SJ. Serum miR-200c expression level as a prognostic biomarker for gastric cancer. *Genet Mol Res* 2015;14:15913-15920.
46. Meng X, Müller V, Milde-Langosch K, Trillsch F, Pantel K, Schwarzenbach H. Circulating cell-free miR-373, miR-200a, miR-200b, and miR-200c in patients with epithelial ovarian cancer. *Adv Exp Med Biol* 2016;924:3-8.
47. Le MT, Hamar P, Guo C, Basar E, Perdigao-Henriques R, Balaj L, Lieberman J. miR-200-containing extracellular vesicles promote breast cancer cell metastasis. *J Clin Invest* 2014;124:5109-5128.
48. Wang K, Zhang S, Marzolf B, Troisch P, Brightman A, Hu Z, Hood LE, Galas DJ. Circulating microRNAs, potential biomarkers for drug-induced liver injury. *Proc Natl Acad Sci U S A* 2009;106:4402-4407.
49. Lewis BP, Burge CB, Bartel DP. Conserved seed pairing, often flanked by adenosines, indicates that thausands of human genes are microRNA targets. *Cell* 2005;120:1-20.
50. Grimson A, Farh KK, Johnston WK, Garrett-Engele P, Lim LP, Bartel DP. MicroRNA targeting specificity in mammals: determinants beyond seed pairing. *Mol Cell* 2007;27:91-105.
51. Chou CH, Chang NW, Shrestha S, Hsu SD, Lin YL, Lee WH, Yang CD, Hong HC, Wei TY, Tu

SJ, Tsai TR, Ho SY, Jian TY, Wu HY, Chen PR, Lin NC, Huang HT, Yang TL, Pai CY, Tai CS, Chen WL, Huang CY, Liu CC, Weng SL, Liao KW, Hsu WL, Huang HD. miRTarBase 2016: updates to the experimentally validated miRNA-target interactions database. *Nucleic Acids Res* 2016;44:D239-D247.

52. Berezikov E, Guryev V, van de Belt J, Wienholds E, Plasterk RH, Cuppen E. Phylogenetic shadowing and computational identification of human microRNA genes. *Cell* 2005;120:21-24.

Figure legends

Figure 1. Expression validation and invasion assays using cells transfected with mimics or inhibitors to miRNAs identified in microarray analyses. **(a)** Validation of miRNA mimic transfection. Cells (8×10^4 cells/well) were cultured in 12-well-plates overnight and then transfected with 0.8 µg miRNA mimic negative control #1 (Bioneer, Alameda, CA; open columns) or mimics for miR-23b-3p, miR-191-5p, miR-200c-3p, miR-221-3p, miR-92b-5p, or miR-185-5p (closed columns) with GeneSilencer siRNA transfection reagent (Genlantis, San Diego, CA) according to the manufacturer's instructions. MicroRNAs were extracted 24 h post-transfection with a High Pure miRNA Isolation Kit (Roche, Mannheim, Germany) and subjected to poly(A) tailing (M0276; New England BioLabs, Ipswich, MA), oligo(dT) adapter annealing, and qPCR with a miRNA EasyScript cDNA synthesis kit (Applied Biological Materials, Richmond, BC, Canada), EvaGreen miRNA qPCR MasterMix (Applied Biological Materials), and LightCycler 480 System (Roche) according to the manufacturer's instructions. *SNORD44* was used as an internal control. miRNA expression was normalized to that of U6-2. **(b)** Three estimated miR-205-5p targets (*TRIB3*, *ERBB3*, and *ZEB1*) and **(c)** three estimated miR-200c-3p targets (*CHD9*, *ETNK1*, and *WRN*) were used to validate the effects of each miRNA inhibitor (Bioneer; closed columns) in SQUU-A and SQUU-B compared to that of miRNA inhibitor negative control #1 (Bioneer; open columns). **(d)** qPCR analysis for *CHD9*, *ETNK1*, and *WRN* in SUQQ-A cells transfected with miR-200c-3p mimic (closed columns) compared to those treated with miRNA mimic negative control #1 (open columns). *S18* was used as an internal control. The mature miRNA mimic and inhibitor sequences are shown in Supplementary Table 2. All experiments were performed in triplicate in three independent experiments. Error bars represent SD. $^{**}P < 0.01$, $^{***}P < 0.001$ versus the corresponding control by Mann-Whitney *U*-test. **(e)** Matrigel invasion assays using miRNA mimics or inhibitors. At 24 h post-transfection, 5×10^4 SQUU-A or SQUU-B cells were subjected to invasion assays as previously described[22], but with a 48-h incubation period. Scale bars: 100 µm. Quantification was performed by counting the number of invasive cells in a visual field at 40-fold magnification. The analysis was performed in triplicate in three independent experiments with four random visual fields per culture insert. Error bars represent SD. $^{***}P < 0.001$ by Mann-Whitney *U*-test).

Figure 2. Invasion assays in SQUU cells with knockdown or overexpression of miR-200c-3p downstream targets. **(a)** Validation of mRNAs in SQUU-A cells 24 h after transfection with *CHD9*, *ETNK1*, or *WRN* siRNA. Total RNA extraction, RT reactions, and real-time PCR were performed as previously reported[22,28]. PCR primer sequences and amplicon sizes are shown in Supplementary Table 1. *GAPDH* was used as an internal control. All experiments were performed in duplicate in three

independent experiments. Error bars represent SD. ***P < 0.001 versus the negative control siRNA by Mann-Whitney U-test. All siRNA sequences (Bioneer) are shown in Supplementary Table 3. **(b)** Validation of protein expression in SQUU-A cells 48 h after siRNA transfection with antibodies directed to CHD9 (Proteintech, Rosemont, IL; 1:2000), ETNK1 (Abgent, San Diego, CA; 1:2000), and WRN (Abgent; 1:2000) as previously reported[28]. HeLa cell extract (DS Pharma Biomedical, Osaka, Japan) was used as a positive control. GAPDH (Acris Antibodies, San Diego, CA; 1:40,000) was used as an internal control. Quantitation of each target expression normalized to that of GAPDH is shown in each lower panel. Each experiment was repeated three times. Data represent the mean ± SD. *P < 0.05 and ***P < 0.001 versus the control. **(c)** Matrigel invasion assay using siRNA transfectants performed as described in Figure 1d. Scale bars: 100 μm. The analysis was performed in triplicate in three independent experiments with four random visual fields per culture insert. Error bars represent SD. ***P < 0.001 by Mann-Whitney U-test. **(d)** Validation of protein expression in SQUU-B cells 48 h after transfection with CHD9, ETNK1, and WRN cDNAs in the pcDNA3.1-C-(k)DYK backbone (GenScript, Tokyo, Japan). Briefly, 8×10^4 cells/well were cultured in a 12-well-plate overnight and transfected with 0.5 μg of each plasmid DNA or pcDNA3.1-C-(k)DYK empty vector control with FuGENE HD Transfection Reagent (Promega, Madison, WI) according to the manufacturer's instructions. Cells were collected 48 h after the transfection. Immunoblot analysis was performed as in (**b**). Quantitation of each target expression (normalized by the amount of GAPDH) in an immunoblot is shown in each lower panel. Each experiment was repeated three times. Data represent the mean ± SD. *P < 0.05 and ***P < 0.001 versus controls. **(e)** Matrigel invasion assay using SQUU-B cells overexpressing CHD9, ETNK1, or WRN as performed in Figure 1d. Scale bars: 100 μm. Analyses were performed in triplicate in three independent experiments with four random visual fields per culture insert. Error bars represent SD. *P < 0.05 and ***P < 0.001 by Mann-Whitney U-test.

Table 1. Differential miRNA expression in ExoB vs ExoA.

Upregulated	Accession No.	Fold Change
hsa-miR-191-5p	MIMAT0000440	31.78
hsa-miR-4454	MIMAT0018976	24.59
hsa-miR-221-3p	MIMAT0000278	20.97
hsa-miR-193b-3p	MIMAT0002819	10.85
hsa-miR-5100	MIMAT0022259	8.40
hsa-miR-1246	MIMAT0005898	7.41
hsa-miR-6875-5p	MIMAT0027650	6.77
hsa-miR-185-5p	MIMAT0000455	5.06
hsa-miR-200c-3p	MIMAT0000617	4.96
hsa-miR-3622a-5p	MIMAT0018003	4.08
hsa-miR-23b-3p	MIMAT0000418	3.32
hsa-miR-3195	MIMAT0015079	2.93
hsa-miR-3197	MIMAT0015082	2.89
hsa-miR-4728-5p	MIMAT0019849	2.48
hsa-miR-7150	MIMAT0028211	2.23
hsa-miR-4640-5p	MIMAT0019699	2.22
hsa-miR-1587	MIMAT0019077	2.20
hsa-miR-92b-5p	MIMAT0004792	2.16
hsa-miR-1910-5p	MIMAT0007884	2.06
has-miR-4443	MIMAT0018961	2.04
hsa-miR-3613-3p	MIMAT0017991	2.00

Downregulated	Accession No.	Fold Change
hsa-miR-4529-3p	MIMAT0019068	0.01
hsa-miR-6840-3p	MIMAT0027583	0.16
hsa-miR-205-5p	MIMAT0000266	0.26
hsa-miR-6790-5p	MIMAT0027480	0.33
hsa-miR-6824-5p	MIMAT0027548	0.34
hsa-miR-3188	MIMAT0015070	0.34
hsa-miR-6716-5p	MIMAT0025844	0.40
hsa-miR-4689	MIMAT0019778	0.42
hsa-miR-6776-5p	MIMAT0027452	0.42
hsa-miR-8075	MIMAT0031002	0.42
hsa-miR-455-3p	MIMAT0004784	0.44

Total RNA was isolated from exosomes purified from SQUU-A (ExoA) and SQUU-B (ExoB) supernatants as previous reported[27,28] using Sepasol-RNA I Super G (Nacalai Tesque, Kyoto, Japan). RNA samples were quantified with an ND-1000 spectrophotometer (NanoDrop, Wilmington, DE) and the quality confirmed with a Experion System (Bio-Rad, Hercules, CA). Total RNA (100 ng) of each sample was labeled using FlashTag™ Biotin HSR RNA Labeling Kit and hybridized to a Affymetrix GeneChip miRNA 4.0 Array according to the manufacturer's instructions. All hybridized microarrays were scanned with an Affymetrix scanner. Relative hybridization intensities and background hybridization values were calculated using Affymetrix Expression Console™. The raw CEL files for gene-level analysis were processed with median polish summarization and quantile normalization in Affymetrix® Transcriptome Analysis Console Software to obtain normalized intensity values. To identify up or down-regulated genes, we calculated ratios (Non-log scaled fold-change ratios were calculated from the ExoA and ExoB normalized intensities to identify upregulated (≥ 2.0-fold) or downregulated (≤ 0.5-fold) genes.

Table 2. Differential mRNA expression in SQUU-A cells treated with ExoB vs ExoA

Upregulated	Accession	Fold Change	Related miRNA
NME3	NM_002513	1.66	-
HSPA1A	DQ409329	1.66	-
ATP1A4	AF459737	1.64	-
CSF1R	M25786	1.57	-
PIP5KL1	NM_001135219	1.51	-
PRKCG	NM_002739	1.50	-
TRIB3	AJ697940	1.50	hsa-miR-205-5p

Downregulated	Accession	Fold Change	Related miRNA
AKT3	AL080074	0.44	hsa-miR-92b-5p
HSPA1B	BC001876	0.49	-
PANK2	BC008667	0.51	hsa-miR-23b-3p
CBWD5	BC043420	0.54	-
CAMK2D	EF139846	0.59	-
MAP3K13	Z25428	0.59	-
CHD9	BC027491	0.60	hsa-miR-200c-3p
ETNK1	NM_001039481	0.61	hsa-miR-200c-3p
WRN	NM_000553	0.61	hsa-miR-200c-3p hsa-miR-221-3p
FRK	NM_002031	0.62	hsa-miR-23b-3p hsa-miR-191-5p
AHSA2	BC050395	0.64	-
FIGN	NM_018086	0.65	-
PIP5K1A	DQ656041	0.65	-
MYO3A	NM_017433	0.66	-
MYO9A	NM_006901	0.66	-

As previously reported[27], we added ExoA and ExoB to SQUU-A cell culture (17.5-fold converted into concentrated supernatant according to our calculation). Total RNA was then isolated from SQUU-A cells treated with ExoA or ExoB for 24 h, using Sepasol-RNA I Super G and purified with an RNeasy Mini Kit (Qiagen, Hilden, Germany) according to the manufacturer's instructions. RNA samples were quantified with an ND-1000 spectrophotometer (NanoDrop) and quality confirmed with a Experion System (Bio-Rad). The cRNA was amplified, labeled using GeneChip® WT Terminal Labeling and Control Kit, and hybridized to Affymetrix Human Transcriptome Array 2.0 according to the manufacturer's instructions. All hybridized microarrays were scanned with an Affymetrix scanner. Relative hybridization intensities and background hybridization values were calculated using Affymetrix Expression Console™. The raw signal intensities of all samples were processed by quantile normalization with Affymetrix® Power Tool version 1.15.0 software. To identify up- or down-regulated genes, we calculated Z-scores and non-log scaled fold-change ratios from the normalized signal intensities of each probe. The criteria for up- or down-regulated genes were as follows: upregulated genes, Z-score ≥ 2.0 and ratio ≥ 1.5-fold; downregulated genes, Z-score ≤ -2.0 and ratio ≤ 0.66. Each related miRNA was searched by miRNA target prediction resources from Affymetrix (Santa Clara, CA) mainly based on miRTarBase[49], microcosm[50], and TargetScan[51,52].

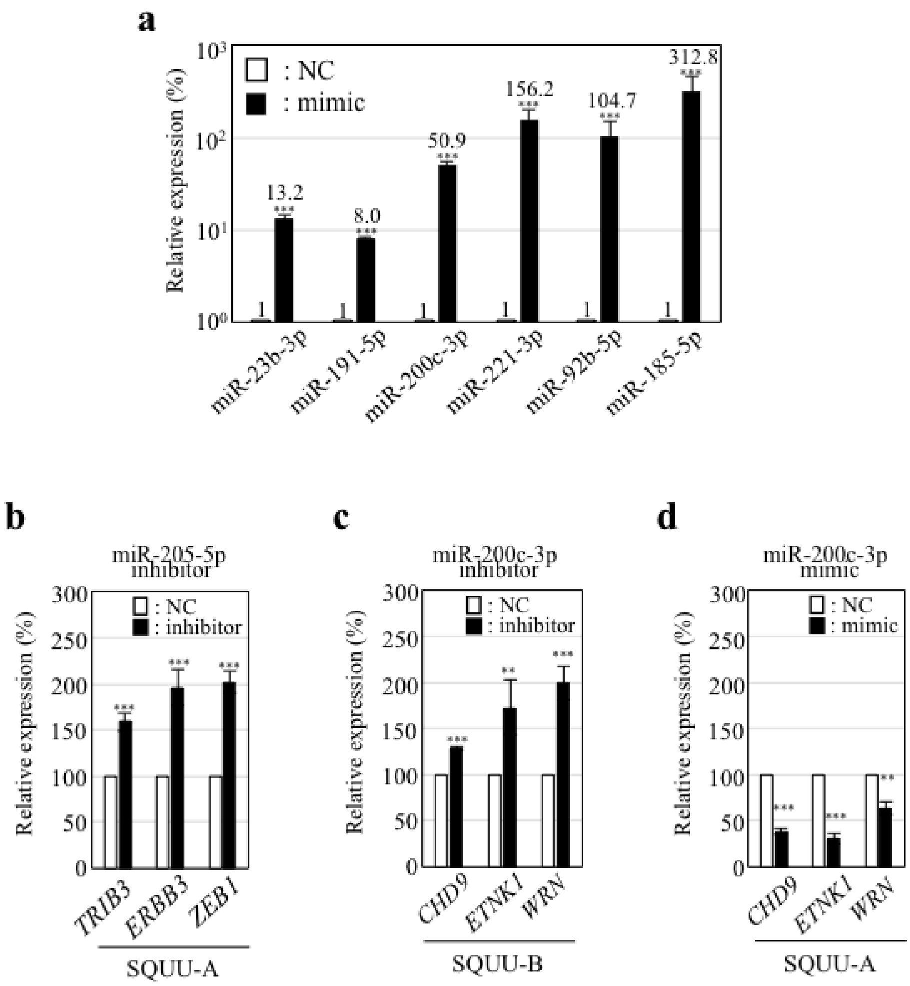

Fig. 1 Kawakubo-Yasukochi *et al*.

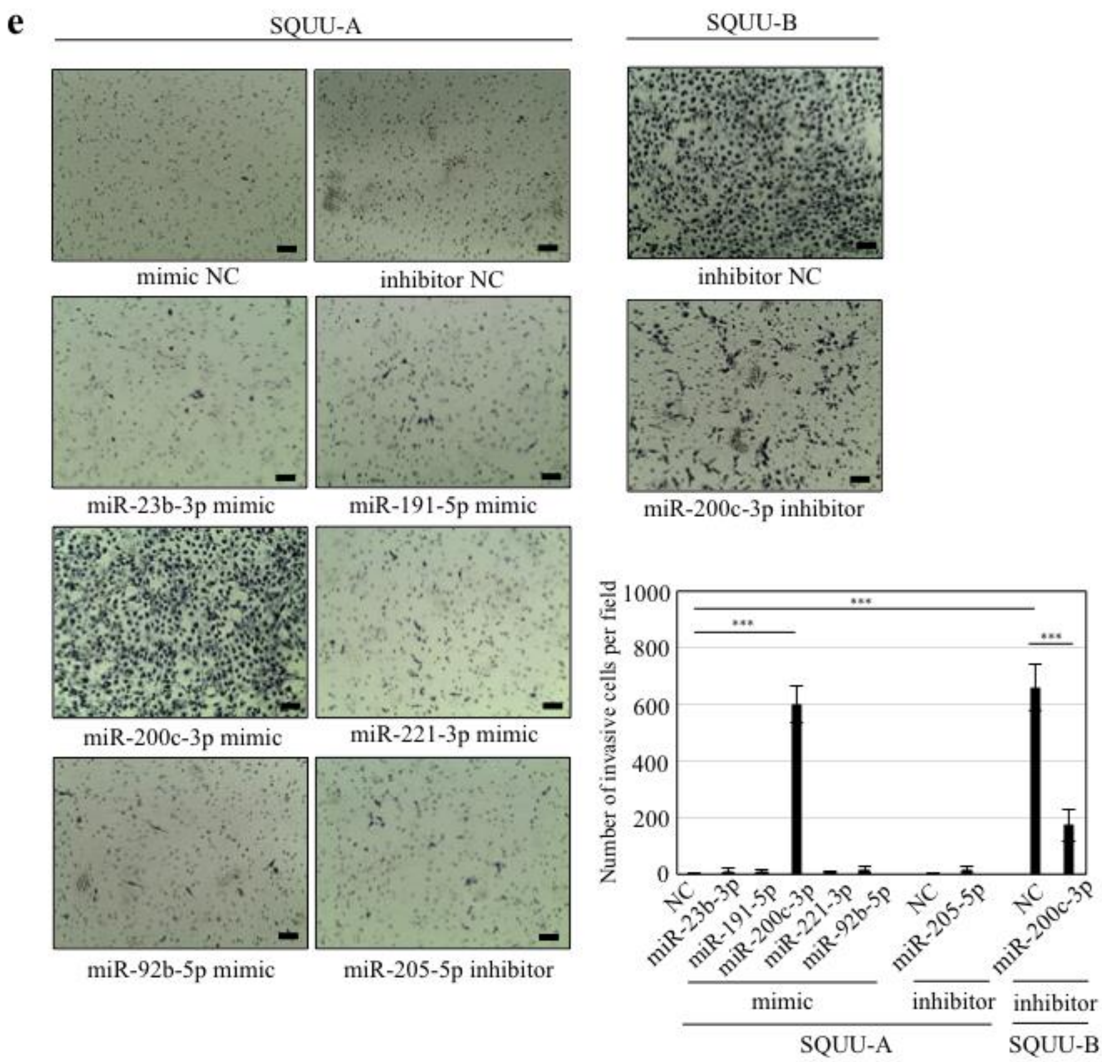

Fig. 1 Kawakubo-Yasukochi *et al*. (continued)

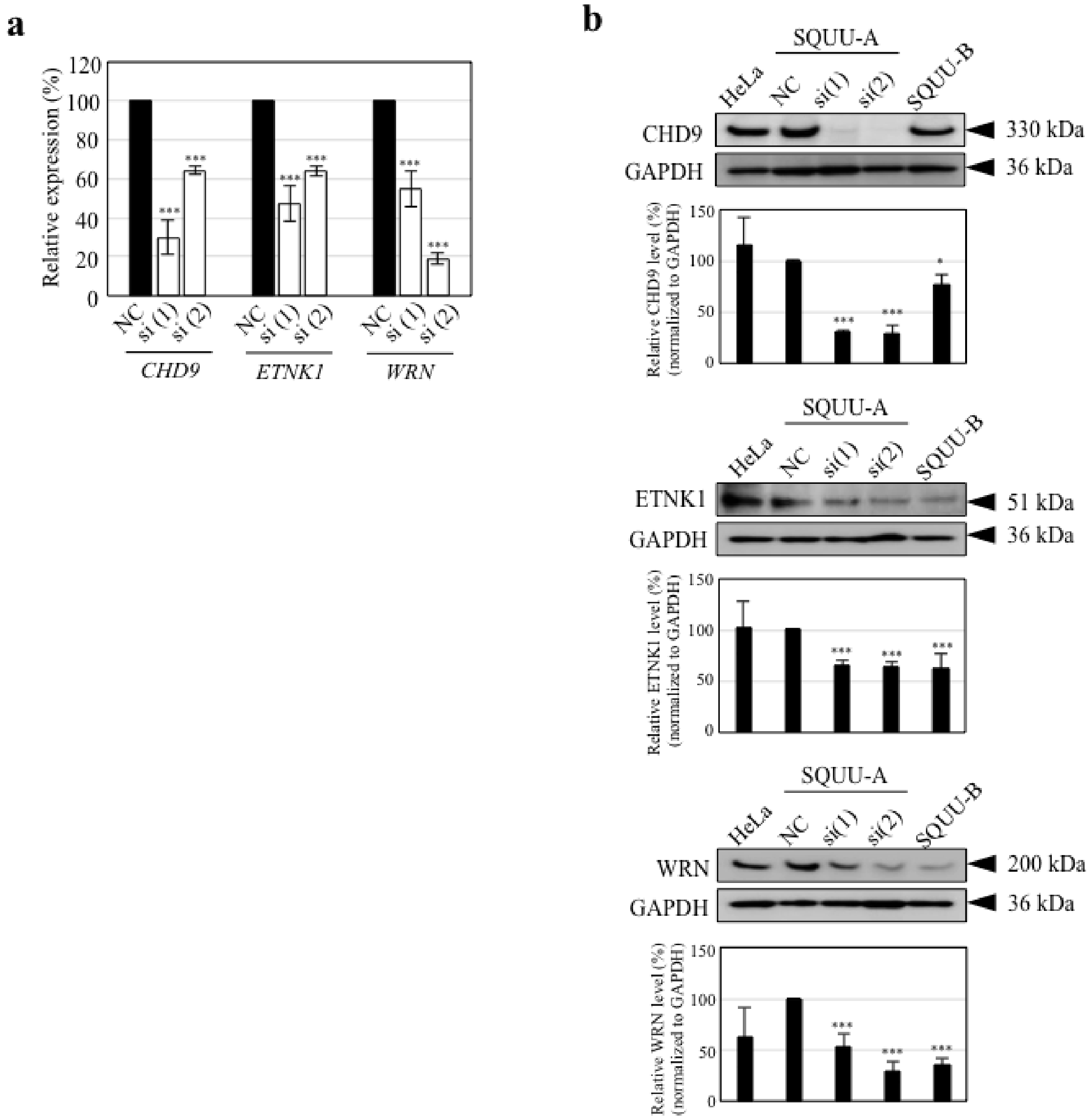

Fig. 2 Kawakubo-Yasukochi *et al.*

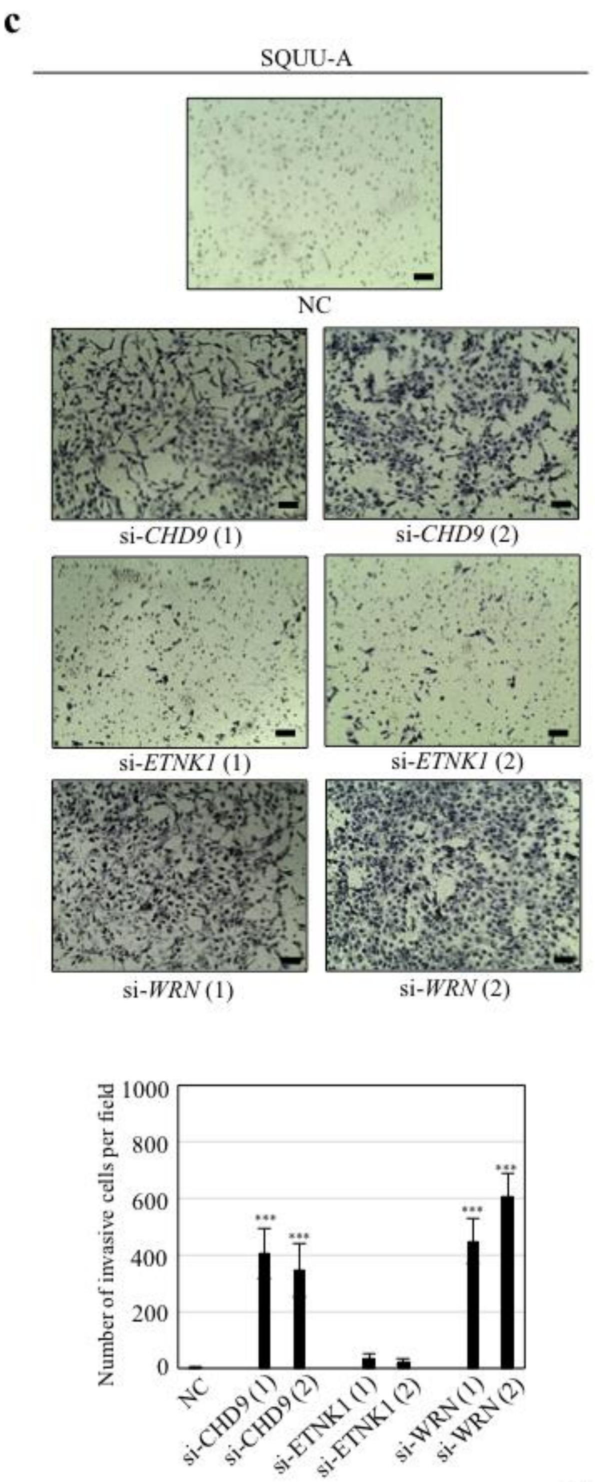

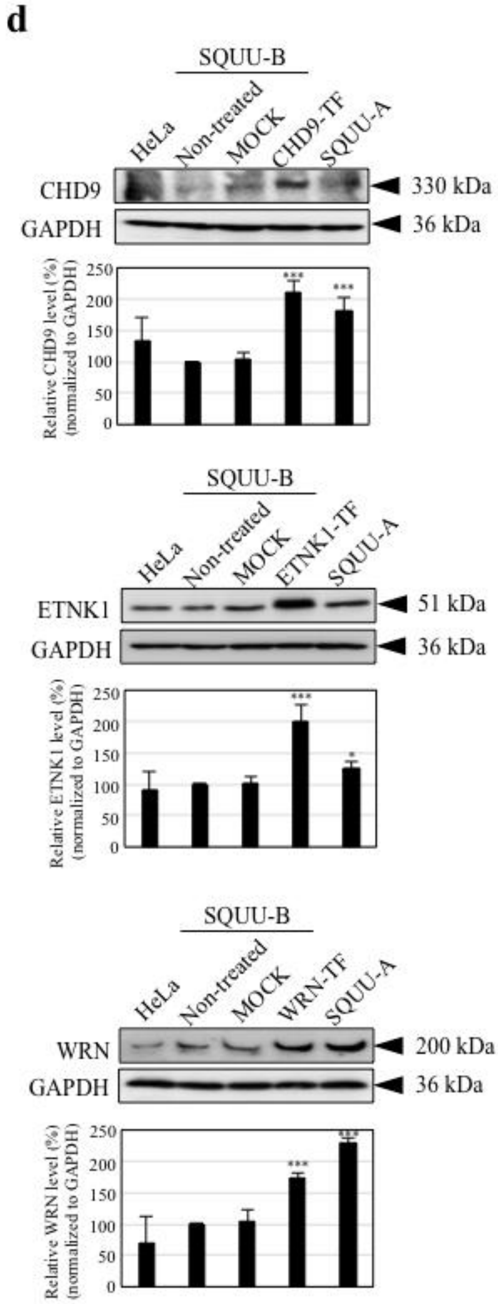

Fig. 2 Kawakubo-Yasukochi *et al.* (continued)

e

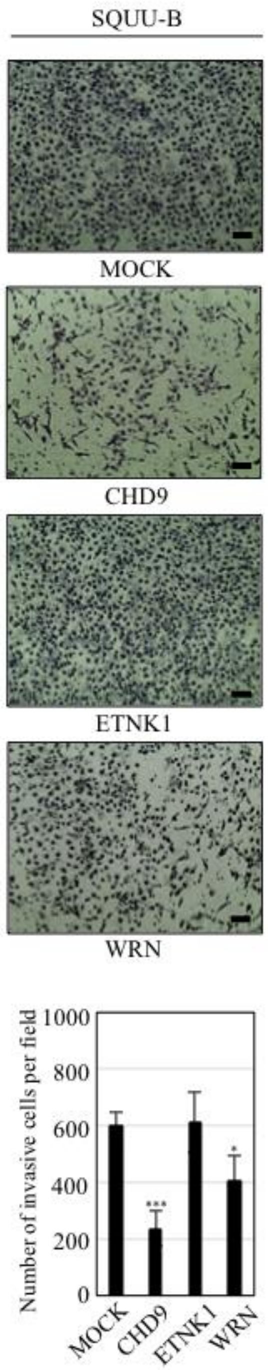

Fig. 2 Kawakubo-Yasukochi *et al*. (continued)

Supplementary information

Exosome-derived miR-200c-3p spreads invasive capacity in human oral squamous cell carcinoma microenvironment

Tomoyo Kawakubo-Yasukochi[1*], Masahiko Morioka[1,2], Mai Hazekawa[1], Atsushi Yasukochi[2], Takuya Nishinakagawa[1], Kazuhiko Ono[1], Shintaro Kawano[2], Seiji Nakamura[2], Manabu Nakashima[1]

[1]Department of Immunological and Molecular Pharmacology, Faculty of Pharmaceutical Science, Fukuoka University, 8-19-1 Nanakuma, Jonan-ku, Fukuoka 814-0180, Japan; [2]Section of Oral and Maxillofacial Oncology, Division of Maxillofacial Diagnostic and Surgical Sciences, Faculty of Dental Science, Kyushu University, 3-1-1 Maidashi, Higashi-ku, Fukuoka 812-8582, Japan

***Correspondence**: Tomoyo Kawakubo-Yasukochi, DDS, PhD, Department of Immunological and Molecular Pharmacology, Faculty of Pharmaceutical Science, Fukuoka University, 8-19-1 Nanakuma, Jonan-ku, Fukuoka 814-0180, Japan, Tel: +81-92-871-6631, Email: tomoyoyasu@fukuoka-u.ac.jp

Supplementary figure legends

Supplementary Figure 1. Matrigel invasion assay in SQUU-A and SQUU-B cells

Matrigel invasion assays were performed as previously reported[22], but with a 48-h incubation time. Scale bars: 100 μm. Quantification was performed by counting the number of invasive cells in a visual field at 40× magnification. Analyses were performed in triplicate in three independent experiments with four random visual fields per culture insert. Error bars represent SD. ***$P < 0.001$ versus SQUU-A controls by Mann-Whitney *U*-test.

Supplementary Figure 2. Validation of microarray results by qRT-PCR.

(a) Validation of exosome-derived miRNAs. miRNA extraction, poly(A) tailing, oligo(dT) adapter annealing, and qPCR were performed as in Figure 1a. *SNORD44* was used as an internal control. miRNA expression was normalized to that of U6-2 (data not shown). Primer sets were purchased from Applied Biological Materials [MPH02300 for miR-200c-3p (accession no. MIMAT00000617), MPH02311 for miR-205-5p (MIMAT00000266), MPH03958 for miR-92b-5p (MIMAT0004792), MPH02365 for miR-23b-3p (MIMAT0000418), MPH02350 for miR-221-3p (MIMAT0000278), MPH02276 for miR-191-5p (MIMAT0000440), MPH00001 for U6-2 (NR_002752), and MPH00003 for SNORD44 (NR_002750)]. ***$P < 0.001$ versus ExoA (open columns) or ExoB (closed columns) by Mann-Whitney *U*-test. **(b)** Validation of mRNAs in SQUU-A cells treated with ExoA or ExoB. Total RNA extraction, RT reaction, and real-time PCR were performed as previously reported[22,28]. PCR primer sequences and amplicon sizes are shown in Supplementary Table 1. All experiments were performed in duplicate in three independent experiments. Error bars represent SD. ***$P < 0.001$ versus SQUU-A cells treated with ExoA (open columns) or ExoB (closed columns) by Mann-Whitney U-test.

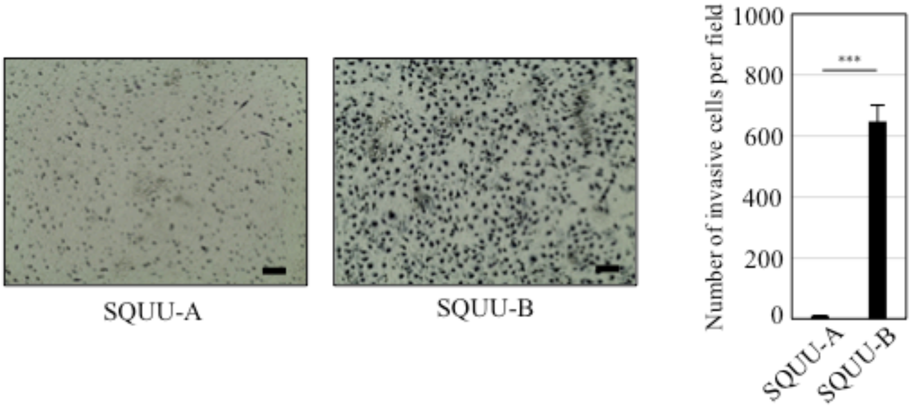

Fig. S1 Kawakubo-Yasukochi *et al*.

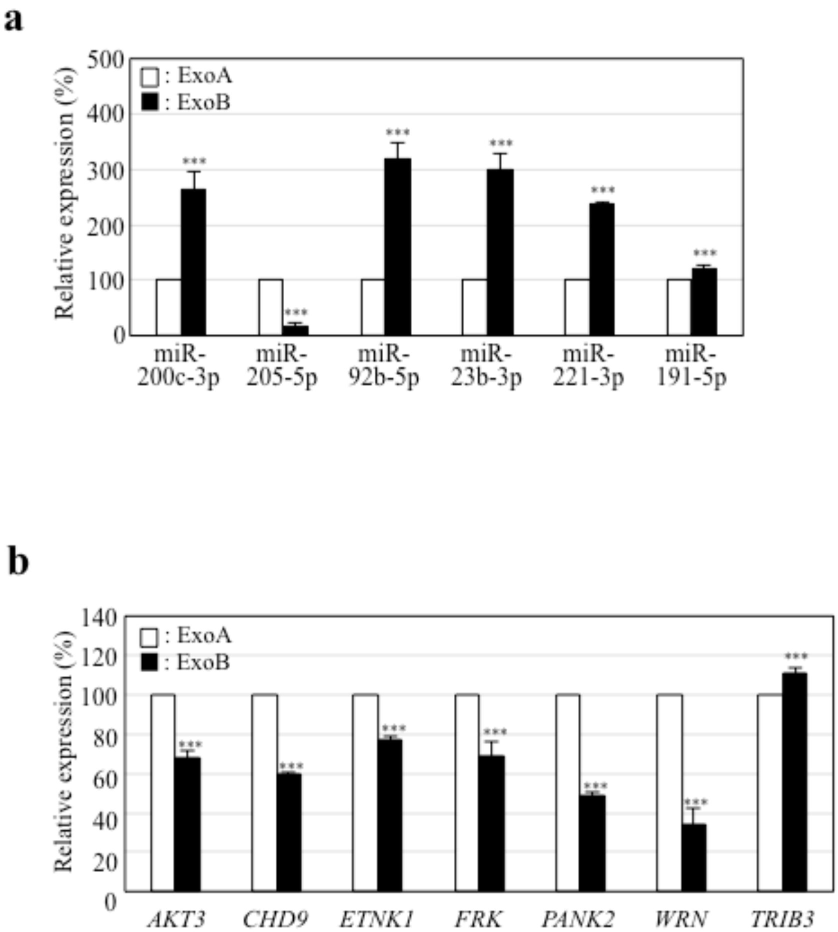

Fig. S2 Kawakubo-Yasukochi *et al*.

Gene (Accession number)	Direction	Primer sequence	Base pairs	Probe
S18 (X03205.1)	Forward Reverse	GCA ATT ATT CCC CAT GAA CG GGG ACT TAA TCA ACG CAA GC	68 bp	48
GAPDH (NM_002046.3)	Forward Reverse	AGC CAC ATC GCT CAG ACA C GCC CAA TAC GAC CAA ATC C	66 bp	60
AKT3 (BC121154.2)	Forward Reverse	TTG CTT TCA GGG CTC TTG AT CAT AAT TTC TTT TGC ATC ATC TGG	75 bp	22
CHD9 (NM_025134.4)	Forward Reverse	TCA TCA GCA TTT ACA TGA CAG AAA CCA GAA CCA TCG CTC TTC TT	78 pb	75
ETNK1 (NM_001039481.1)	Forward Reverse	AGC CTC CTG CAA CAC CTG TGT GAT TCC ATC TGT GAA GAG C	75 bp	79
FRK (BC012916.1)	Forward Reverse	CTG GGG AAA CCA TGC TTA AA GGT CCA CGG TTT TAT ACG ACA	67 bp	33
PANK2 (AF494409.1)	Forward Reverse	TGG AGG TGG AGC GTA CAA AT TTG CAA AGC TGA AGA TCA CC	63 bp	15
WRN (NM_000553.4)	Forward Reverse	GAC AGA TGT TGC CAA TAA AAA GC TCA GGA GCT GTT TAC CTA AGA GG	89 bp	1
TRIB3 (NM_021158.3)	Forward Reverse	GTC TTC GCT GAC CGT GAG A CAG TCA GCA CGC AGG AGT C	67 bp	67
ERBB3 (M29366.1)	Forward Reverse	CTG ATC ACC GGC CTC AAT GGA AGA CAT TGA GCT TCT CTG G	73 bp	37
ZEB1 (NM_001128128.2)	Forward Reverse	TGT TAC CAG GGA GGA GCA GT TGC CCT TCC TTT CCT GTG T	76 bp	3

Supplementary Table 1. Primer sets and probe numbers for qPCR analysis. TaqMan probes specific for each sequence were selected from the LightCycler Universal Library (Roche)

miRNA mimic for	Mature sequence
miR-23b-3p	AUC ACA UUG CCA GGG AUU ACC
miR-191-5p	CAA CGG AAU CCC AAA AGC AGC UG
miR-200c-3p	UAA UAC UGC CGG GUA AUG AUG GA
miR-221-3p	AGC UAC AUU GUC UGC UGG GUU UC
miR-92b-5p	AGG GAC GGG ACG CGG UGC AGU G
miR-185-5p	UGG AGA GAA AGG CAG UUC CUG A

miRNA inhibitor for	Mature sequence
miR-200c-3p	UAA UAC UGC CGG GUA AUG AUG GA
miR-205-5p	UCC UUC AUU CCA CCG GAG UCU G

Supplementary Table 2. Mature sequences (5'-3') of miRNA mimics or inhibitors. All oligonucleotides were synthesized and validated by BIONEER.

Target mRNA	Direction	Sequence
CHD9 (1)	Sense	CUG GUA ACU CGU AAC UCA U (dTdT)
	Antisense	AUG AGU UAC GAG UUA CCA G (dTdT)
CHD9 (2)	Sense	CUG GAU UAC CAA AUC UGU U (dTdT)
	Antisense	AAC AGA UUU GGU AAU CCA G (dTdT)
ETNK1 (1)	Sense	CAC AAC UCU ACU GUA CCU U (dTdT)
	Antisense	AAG GUA CAG UAG AGU UGU G (dTdT)
ETNK1 (2)	Sense	CCA CAA CUC UAC UGU ACC U (dTdT)
	Antisense	AGG UAC AGU AGA GUU GUG G (dTdT)
WRN (1)	Sense	GAG CCU UAA CAG UCU GGU U (dTdT)
	Antisense	AAC CAG ACU GUU AAG GCU C (dTdT)
WRN (2)	Sense	CUA CUU AGC GAC AUG AAC A (dTdT)
	Antisense	UGU UCA UGU CGC UAA GUA G (dTdT)

Supplementary Table 3. siRNA oligonucleotide sequences (5'-3'). The siRNA oligonucleotides were synthesized and validated by BIONEER.